11th International Conference on Vibration Problems
Z. Dimitrovová *et.al.* (eds.)
Lisbon, Portugal, 9–12 September 2013

VIBRATION CONTROL OF TENSION-ALIGNED STRUCTURES

Alejandro R. Diaz*, Ranjan Mukherjee, Tingli Cai

Department of Mechanical Enineering
Michigan State University
East Lansing, Michigan, USA
{diaz, mukherji, caitingl}@egr.msu.edu

Keywords: Vibration Suppression, Tension

Abstract. *Large space structures are being considered to support radar antennas for imagery and moving object identification, solar arrays for energy collection, and platforms for large mirrors and telescopes. In these applications such structures have stringent design requirements in terms of precision, environmental stability and durability, high deployment reliability, manufacturability, and cost. In particular, high precision is particularly difficult to achieve since these structures are sensitive to vibration sources located on the structure. Vibration sources can transmit vibration from one location in the structure to another and cause misalignment of sensitive instruments. Vibration suppression in large space structures is a challenging task for engineers.*

Recently, tension-aligned structures have been proposed for space applications where high precision is an important consideration. A tension-aligned structure, analogous to a bow with a string, consists of a support structure in compression and a sensor array in tension. By providing larger stiffness for a lower mass, tension-aligned structures have better packaging efficiency and maintain flatness of the sensor surface. This work presents an efficient method for vibration suppression in a tension-aligned array structure using constraint actuators. The primary role of constraint actuators is to cyclically apply and remove constraints such that vibration energy is efficiently funneled into high-frequency modes of the structure, where it can be dissipated quickly and naturally due to high rates of damping. A cycle of constraint application and removal can never add energy and hence the method can potentially achieve vibration control without accurate knowledge of the system states. The vibration control methodology is applied to a tension-aligned array structure supported by a structure in compression. This approach for vibration suppression has the potential to positively influence the development of tension-aligned architectures which are contemplated for large precision apertures in space.

1 INTRODUCTION

Large space structures are being considered as sensorcraft for imagery and moving object identification and tracking, solar arrays for energy collection, and platforms for long aperture mirrors and telescopes. These structures usually consist of a large support substructure and a phased array antennas attached to it [1]. A series of stringent design requirements need to be met when developing space structures, such as precision, environmental stability and durability, high packaging efficiency and deployment reliability, manufacturability, and cost. Among these requirements, high precision is particularly difficult to achieve since large structures are sensitive to disturbances that result in vibration. Caused by various sources including slewing load, thermal excursion, dynamic excitation from reaction resonance [2], vibration can be transmitted from one location in the structure to another and can cause misalignment of sensitive instruments which degrades system performance. Vibration suppression in large space structures poses serious challenges for engineers.

Because of their architecture, the main form of deformation in these systems is low-frequency out-of-plane vibration of array antennas. As the dimension of the structure increases, in order to suppress vibration in the out-of-plane direction, bending stiffness of the structure needs to be increased accordingly. In traditional solutions such as DARPA's ISAT program [3], large deployable truss-like support structures were developed to provide sufficient bending stiffness. This inevitably increases the depth of the system and reduces both packaging efficiency and deployment reliability. Besides that, deep structures suffer from thermal deformation [4]. Such limitations in traditional designs call for innovative and practical solutions.

Tension-aligned structures have been proposed for space applications where high precision is an important consideration [5, 6]. Analogous to a bow with a string, in a tension-aligned structure, array antennas are not attached to the support structure, but connected to it via tensioners at each end (see Figure 1). The support structure functions as a compressive member to provide tension to array antennas. The tension in the antenna array helps maintain flatness and increases the out-of-plane geometric stiffness of the sensor surface. Tension also increases structural damping [7] which facilitates vibration suppression. Other benefits of tension-aligned structures include elimination of accuracy requirements of the support structure, since the contact area with array antennas is much reduced; better packaging efficiency because the support structure and the array antennas can be packaged and deployed separately, and also because

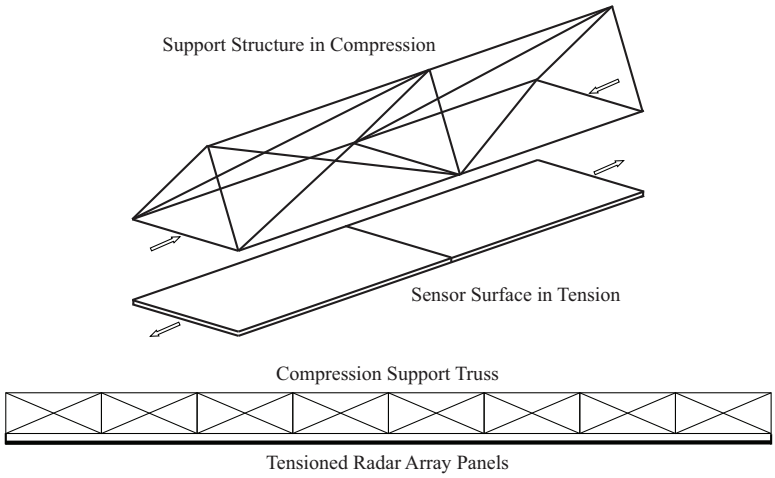

Figure 1: A tension-aligned structure comprised of a support structure and a sensor surface - taken from [6]

less mass is needed to provide the same stiffness; reduced nonlinear effect such as deadband [6] and compensation for manufacturing errors [8]. The tension-aligned architecture considered for antennas as panel arrays is equally suited for radar designs involving flexible membranes [9].

Tension-aligned systems proposed so far mostly treat tension as a passive mechanism for vibration control. Passive control may not be efficient enough for applications with the accuracy requirement set by ISAT programs, and the tension imparted may be too high to achieve the required level of stiffness. High tension levels are usually not suitable for long-term tasks. On the other hand, active control methods, if considered, often employ sensors located through the structure. Control strategy is formulated based on accurate mathematical modelling. Feedback is then implemented through actuators operated by on-line controllers. For space structures, such modeling and computation can be very complex and large-scale. Active methods sometimes suffer from stability issues, because actuators may add energy to the structure if modeling or implementation is problematic. With these considerations in mind, the authors seek a compromise between passive and active control methods.

A semi-active control method for tension-aligned structures is proposed in this paper. The core idea of our method is based on the concept of stiffness variation. To vary the stiffness of the structure, the method applies and removes constraints cyclically. As a consequence of such operation, vibration energy is funneled into the high-frequency modes of the structure, where it can be dissipated quickly and naturally due to high rates of internal damping. This semi-active method requires very few sensors and actuators. It employs a simple control strategy which eliminates the need for large-scale modeling and computations, and it has the advantage of robustness because actuators will never add energy to the system or cause instability.

Stiffness variation as a method for vibration suppression has been investigated by several researchers [10, 11, 12, 13, 14]. In those works, active variable-stiffness elements are placed in the structure to store and release elastic energy. In contrast, in our earlier work [15, 16, 17], direct energy release in those active members through stiffness variation was not the main reason for system energy loss. The action of stiffness variation, i.e., applying or removing constraints, does not change the system energy noticeably. Energy dissipation was accomplished instead through a targeted energy redistribution from low-frequency modes to high-frequency modes where internal damping plays an essential role for vibration suppression. This paper, as an extension of our earlier work, applies such control methodology to a simple tension-aligned structure.

2 MODEL OF A SIMPLE TENSION-ALIGNED STRUCTURE

In this section the finite-element model of a simple tension-aligned structure is presented. This tension-aligned structure, shown in Figure 2, consists of a planar elastica arch that functions as a support structure in compression; and a hinged panel array in tension. The arch is slender and initially curved to form the arc of a circle. Under eccentric compressive end loads the arch is nonlinearly deformed. Its loads are in equilibrium with the tension forces applied on the panels.

2.1 Support Structure - A Planar Elastica Arch

The truss-like support structure is simplified into a planar elastica arch. The dynamic model of the arch is obtained based on the work by Perkins [18]. Shown in Figure 3, before deformation, the arch is initially an arc of a circle with the curvature of k_0. It is then held in static equilibrium under the horizontal end-load f and moment fd, where d denotes the vertical eccen-

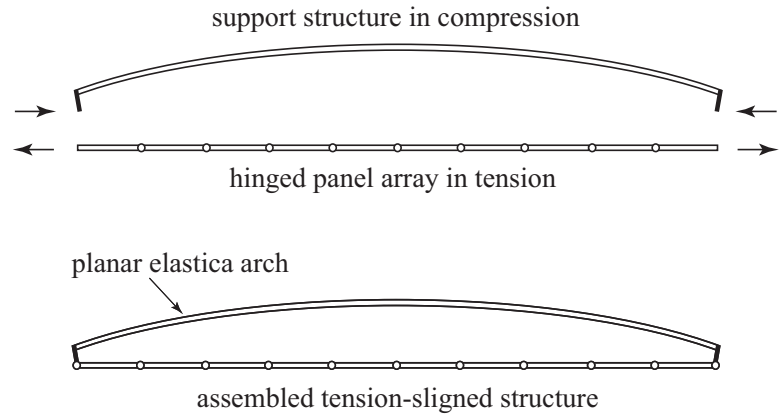

Figure 2: A tension-aligned structure formed by connecting a support structure (in compression) to an array of hinged panels (in tension)

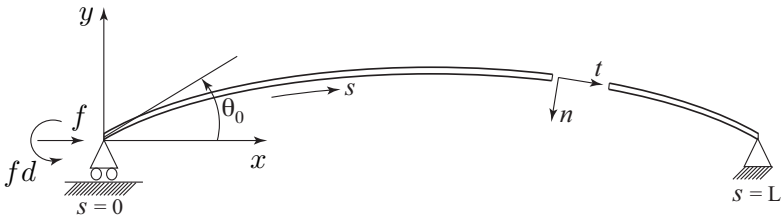

Figure 3: A planar elastica arch

tricity of the end-load f. The arc length of the arch is assumed to be L in the static equilibrium state. The strain energy of the arch can be expressed as

$$\Pi_V = \frac{1}{2}\int_0^L \left(EI(k-k_0)^2 + EAe^2\right)\,\mathrm{d}s \tag{1}$$

where constants E, A and I are Young's modulus, cross-sectional area, and area moment of inertia of the arch, respectively; k and e are deformed the curvature and axial strain along the centerline, respectively. We follow the expressions for k and e derived by Perkins and Mote [19] as:

$$k = k_s + \frac{\partial}{\partial s}\left(\frac{\partial u_n}{\partial s} + k_s u_t\right) \tag{2}$$

$$e = \frac{p}{EA} = \frac{p_s}{EA} + \frac{\partial u_t}{\partial s} - k_s u_n + \frac{1}{2}\left[\left(\frac{\partial u_t}{\partial s} - k_s u_n\right)^2 + \left(\frac{\partial u_n}{\partial s} + k_s u_t\right)^2\right] \tag{3}$$

where p is the time-varying axial force along the arch's centerline; subscript s indicates the static values of p and k, measured in the static equilibrium configuration; u_t and u_t are tangential and normal components of displacements using a fixed frame built along the centerline of the arch's static equilibrium shape. FEM is used to discretized the arch. After carrying out a nonlinear static analysis, the vibration model of the arch is then obtained upon the linearization around the static equilibrium shape.

2.2 Hinged Panel Array

The hinged panel array, shown in Figure 4, is modeled using frame elements. Each element has two nodes and three degrees of freedom at each node: two translational and one rotational

Figure 4: The array of hinged panels

degrees of freedom. A hinge between two neighboring panels is treated as a node after meshing. Elements on the left and right sides of the hinge node share the translations of that node but have independent rotations on the hinge node. In order to take the effect of tension into account, a geometric stiffness matrix is added to the standard frame stiffness matrix.

3 STIFFNESS VARIATION IN MULTI-DOF SYSTEMS

3.1 Stiffness Variation and Modal Disparity

Consider the N-DOF linear system

$$\mathbb{M}\ddot{X} + [\mathbb{K}_0 + \Delta\mathbb{K}(t)]X = 0 \tag{4}$$

where $X = (X_1, X_2, \cdots, X_N)^T$ denotes the vector of generalized coordinates, $\mathbb{M}$ is the mass matrix. In Eq. 4, the system has the stiffness consisting of two terms: a constant stiffness matrix $\mathbb{K}_0$ and a time-varying stiffness matrix $\Delta\mathbb{K}(t)$ which is further described as

$$\Delta\mathbb{K}(t) = \begin{cases} 0 & \text{if } t \in [t_i, t_{i+1}), \quad \text{unconstrained state} \\ K_r & \text{if } t \in [t_{i+1}, t_{i+2}), \quad \text{constrained state} \end{cases}, \qquad i = 0, 2, 4, \cdots \tag{5}$$

where t_j, $j = 1, 3, 5, \cdots$, are chosen such that the change in stiffness does not increase the total energy of the system. In Eq.(5), the change in the stiffness matrix can be viewed as addition and removal of massless springs connecting pairs of generalized coordinates. When such springs are added, we call the system in constrained state; when the springs are removed, we call the system in unconstrained state.

Let scalars μ_i and vectors ϕ_i, $i = 1, 2, \ldots, N$ denote modal coordinates and the corresponding mode shapes that are mutually orthogonal to each other in the unconstrained state. Similarly, let scalars ν_i and vectors ψ_i, $i = 1, 2, \ldots, N$ denote modal coordinates and the corresponding mode shapes that are mutually orthogonal to each other in the constrained state. ϕ_i and ψ_i are normalized with respect to the mass matrix $\mathbb{M}$. The transitions of the system between the unconstrained state and the constrained state need to guarantee that there is no discontinuity in displacements and velocities of the general coordinates. Such transitions can be described by the relations

$$\nu(t_{i+1}) = \Gamma\mu(t_{i+1}) \tag{6}$$
$$\dot{\nu}(t_{i+1}) = \Gamma\dot{\mu}(t_{i+1}) \tag{7}$$
$$\mu(t_i) = \Gamma^T\nu(t_i) \tag{8}$$
$$\dot{\mu}(t_i) = \Gamma^T\dot{\nu}(t_i) \tag{9}$$

where $i = 0, 2, 4, \cdots$, μ and ν are vectors of modal coordinates. In Eq. 6-9, Γ is the so-called modal disparity matrix [20, 21], which is given by the relation

$$\Gamma = \Psi^T\mathbb{M}\Phi \tag{10}$$

where $\Phi = [\phi_1, \phi_2, \ldots, \phi_N]$ and $\Psi = [\psi_1, \psi_2, \ldots, \psi_N]$ are modal matrices in the unconstrained and constrained states, respectively.

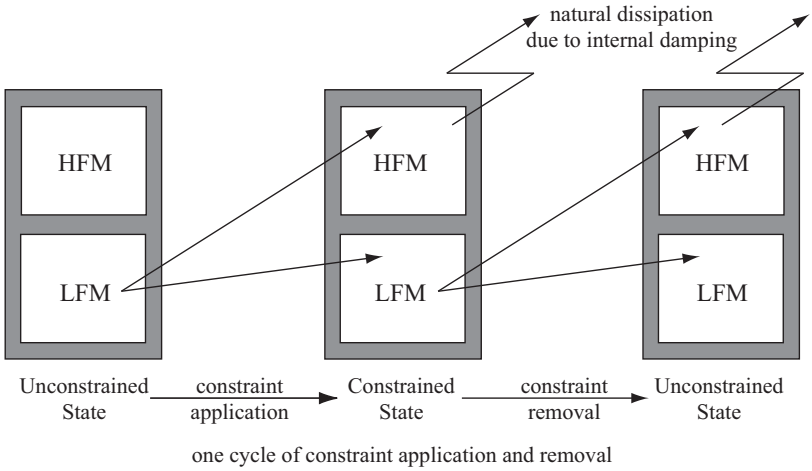

Figure 5: Vibration suppression through energy funneling from low-frequency modes (LFM) into high-frequency modes (HFM)

When $K_r = 0$, *i.e.*, when no stiffness variation is introduced, the modal disparity matrix Γ is the identity matrix. When $K_r \neq 0$, Γ must have nonzero off-diagonal entries, i.e., $\Gamma(i,j) \neq 0$ for some values of i and j, $i \neq j$. This means that energy will be transferred from the j-th mode of the unconstrained state to the i-th mode of the constrained state, and vice versa. If energy is transferred from a low frequency mode in one state to a high frequency mode in another state, it will then be dissipated quickly. Modal damping can be assumed in this model where damping rate of each mode is proportional to its natural frequency. For the process to be repeated, the system has to be switched back and forth between the constrained state and the unconstrained state. The system should be held for a time period after each switch such that energy in the high-frequency modes is sufficiently dissipated. This strategy for vibration suppression is illustrated in Figure 5.

3.2 Method of Stiffness Variation in Tension-Aligned System

Stiffness variation described by Eq.(5) is implemented in the assembled tension-aligned structure by applying and removing large rotational springs at chosen hinges, as shown in Figure 6. The rotational degrees of freedom of two neighboring panels at a chosen hinge, θ_P^k and θ_P^{k+1}, are connected by a rotational spring with time-varying stiffness. The control logic is designed in such a way that the spring is added when $\theta_P^k(t) - \theta_P^{k+1}(t) = 0$, and is removed after a time period so that energy in the high-frequency modes is estimated to be dissipated. It is apparent that such control logic will never add energy to the system or cause stability issue. In practice, the rotational springs can be realized using electromagnetic brakes.

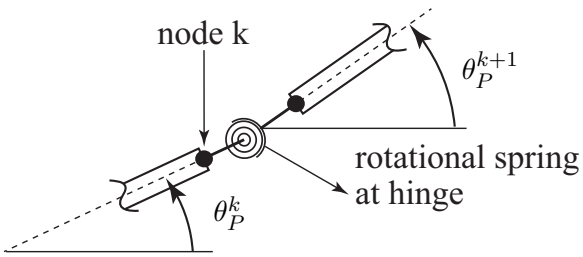

Figure 6: Stiffness variation in the tension-aligned structure is realized using rotational spring

Table 1: Properties of Simulated Tension-Aligned Structure

Material	Aluminum
Young's modulus E	69×10^9 Pa
Density ρ	2700 kg/m^3
Damping ratio ζ	0.001
Panel number	8
Panel length L_{p}	1.000 m
Panel area $b \times h$	0.500 m $\times$ 0.010 m
Cross-section area of support arch A	1.571×10^{-3} m^2
Area moment of inertia of support arch I	1.963×10^{-6} m^4
Maximum height of support arch H_a	0.800 m
Span length of support arch S_a	8.000 m
Arc length of support arch L	8.212 m
Eccentricity of connection d	0.200 m
Tension f	400 N

4 NUMERICAL SIMULATION

The material and geometric properties of the tension-aligned structure are provided in Table 1. Material of the structure is assumed to be aluminum. The damping ratio of all modes is assumed to be $\zeta = 0.001$. The panel array with pre-tension $f = 400$ N applied, is comprised of eight panels with dimensions $L_{\mathrm{p}} \times b \times h$, as illustrated in Figure 7. Each panel is modeled using 10 frame elements. The support structure (elastica arch) is initially an arc of a circle of radius $R = 10.8$ m. Before deformation, the arch has the maximum height of $H_a = 0.8$ m and the span length of $S_a = 8$ m. Its cross-section dimensions are also shown in Table 1. When held in equilibrium, the arch has the arc length of 8.212 m. Compared to the undeformed shape, changes in arc length and span length due to the load are no greater than 0.015 m. The eccentricity d of the load f applied to the support structure is 0.200 m. The arch is modeled using 80 elements.

We simulate the behavior of the structure with and without control, given initial displacements caused by a disturbance. This initial condition are created by displacing the second joint of the hinged panel array (see Figure 7) by 0.08 m (1% of the length of the panel array) transversely and then releasing the structure. Care was taken such that no rigid-body motion is excited. The first 25 modes of the structure were simulated; these again do not include the rigid-body modes. The energy decay of the tension-aligned structure is shown in Figure 8 for three different cases, as described below:

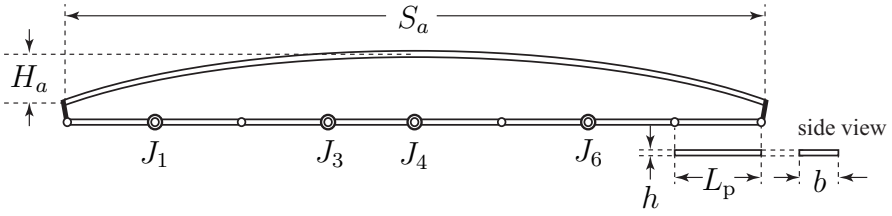

Figure 7: The eight-panel tension-aligned structure used in simulations, both for low-tension and high-tension

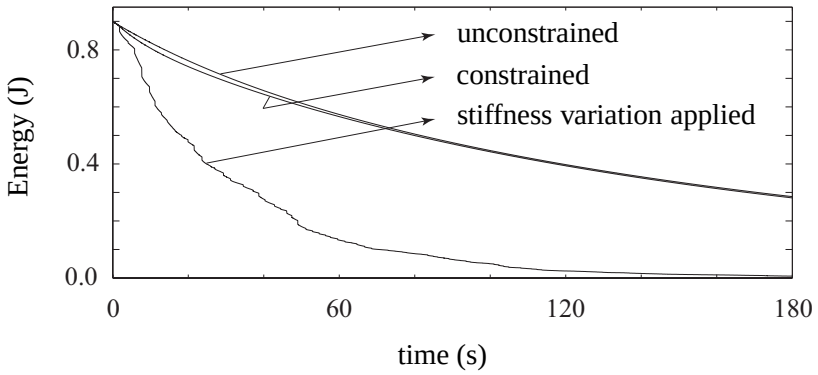

Figure 8: Plot of energy for the three cases

1. Unconstrained structure undergoing free vibration.
2. Constrained structure undergoing free vibration. The structure is referred to as constrained since there are high-stiffness rotational springs applied at joints J_1, J_3, J_4 and J_6 - see Figure 7. As described before, the control logic switches the stiffness of the rotational springs to be activated when the adjacent panels are aligned. The rotational springs are activated sequentially at the earliest possible opportunity and are then kept in their high stiffness state all the time.
3. Structure with controlled stiffness variation. The high-stiffness rotational springs in joints J_1, J_3, J_4 and J_6 are activated sequentially when their adjacent panels are aligned and their stiffness is then set to zero simultaneously. Each change of stiffness occurs at least 0.2 s after the previous one, so that energy in high-frequency modes can be dissipated sufficiently. The cyclical process is repeated for 128 times in the simulation period of 180 sec.

It is clear from Figure 8 that in the cases of unconstrained structure and constrained structure energy decays much more slowly compared to the case of structure with controlled stiffness variation. After 180 sec, the unconstrained structure and the constrained structure have 31.8% and 31.3% of their initial energy left, respectively; in contrast, the structure with controlled stiffness variation has 0.7% of its initial energy left. Although vibration energy is dissipated through internal damping in all three cases, the structure with controlled stiffness variation has higher rate of energy dissipation since it effectively funnels energy from the low-frequency modes to the high-frequency modes.

For the structure with switched stiffness, when the rotational springs are removed simultaneously, residual energy stored in the springs are released instantaneous out from the system. This discontinuous change in the energy, is however not the main mechanism of energy dissipation. The main mechanism, as shown in Figure 8 in the case of controlled stiffness variation applied,

Table 2: First six natural frequencies of the unconstrained and the constrained tension-aligned structure in rad/s for the low-tension case

Unconstrained	ω_1	ω_2	ω_3	ω_4	ω_5	ω_6
	2.151	4.384	6.781	9.416	12.307	15.295
Constrained	$\bar{\omega}_1$	$\bar{\omega}_2$	$\bar{\omega}_3$	$\bar{\omega}_4$	$\bar{\omega}_5$	$\bar{\omega}_6$
	2.231	4.705	8.033	24.911	46.402	58.134

is the effective increase in energy decay rates after each action of stiffness variation, which indicates energy dissipation occurs in high-frequency modes of the system. It also should be noted that since the structure has many degrees-of-freedom, activating the springs in four joints only makes it marginally stiffer than the unconstrained structure. This can be verified from Table 2 which compares the first six natural frequencies of the unconstrained and constrained structures. Yet elevating natural frequencies of the system by this amount is not effective for the purpose of vibration control. As shown in Figure 8, the cases of unconstrained structure and constrained structure energy decays similarly slowly. Vibration suppression needs to be achieved through cyclical control of stiffness variation of the structure.

5 OTHER CONTROL STRATEGIES

There are many control strategies to be explored for vibration control in tension-aligned structures. Following the method presented in this paper, stiffness variation can also be created by placing a translational spring between the support structure and the hinged panel array, as shown in Figure 9. Time-varying stiffness of the translational spring causes the stiffness variation of the structure.

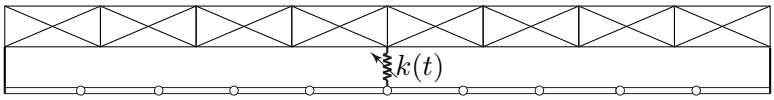

Figure 9: A translational spring with time-varying stiffness $k(t)$ in the tension-aligned structure

Similarly, a spring with time-varying stiffness can be used in connecting the panel array to the end of the support structure. This spring varies axial stiffness of the panel array, as depicted in Figure 10.

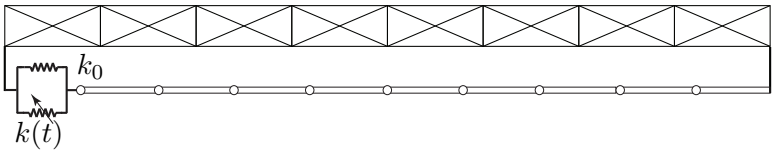

Figure 10: A spring with time-varying stiffness $k(t)$ connecting hinged panels to the end of the support structure

Since tension adds geometric stiffness to hinged panels, changing tension $f(t)$ imparted in panels as shown in Figure 11, is equivalent to varying total stiffness of the structure.

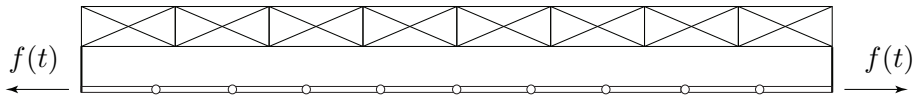

Figure 11: Varying tension in hinged panels

Another way of stiffness variation can be implemented using a sliding mechanism inside the structure, as shown in Figure 12. A slider with prescribed velocity $v(t)$ keeps changing the contact point with the structure, thus creates stiffness variation.

Different strategies of stiffness variation for the purpose of vibration control have different efficiencies. To investigate this furthermore calls for quantitative evaluation of stiffness variation, which leaves an open optimization problem to researchers.

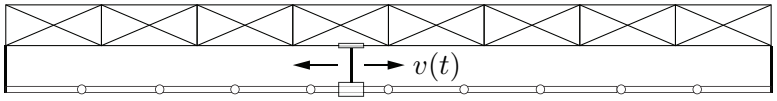

Figure 12: A sliding mechanism inside the structure for stiffness variation

6 CONCLUSIONS

- A simple tension-aligned system was modeled using FEM. The system consists of a planar elastica arch as support structure in compression and a hinged panel array in tension.
- Stiffness variation as a control strategy is presented as an efficient method for vibration suppression in the tension-aligned system.
- This semi-active method requires very few sensors and actuators and eliminates the need for extensive on-line computation based on mathematical modeling. This approach for vibration suppression has the potential to positively influence the development of tension-aligned architectures which are contemplated for large precision apertures in space.

REFERENCES

[1] Lane, S. A., Murphey, T. W. and Zatman, M., 2011, "Overview of the Innovative Space-Based Radar Antenna Technology Program", *Journal of Space and Rockets,* **48**(1), pp.135-145.

[2] Adler, A., Mikulas, M. M., Hedgepeth, J. M., Stallard, M., and Garnham, J., 1998, "Novel Phased Array Antenna Structure Design", *IEEE Aerospace Conference*, Aspen, CO.

[3] Guerci, J. and Jaska, E., 2003, "ISAT - Innovative Space-Based-Radar Antenna Technology", *IEEE International Symposium on Phased Array Systems and Technology,* Honolulu, HI.

[4] Jeon S. K. and Murphey, T. W., 2012, "Fundamental Design of Tensioned Precision Deployable Space Structures Applied to an X-Band Phased Array", *53rd AIAA Structures, Structural Dynamics, and Materials Conference,* Schaumburg, IL.

[5] Mikulas. M., Murphey T., and Jones T. C., 2008, "Tension-Aligned Deployable Structures for Large 1-D and 2-D Array Applications", *49th AIAA Structures, Structural Dynamics, and Materials Conference,* Schaumburg, IL.

[6] Jones. T. C., Waston J. J., Mikulas M., and Bart-Smith H., 2008, "Design and Analysis of Tension-Aligned Large Aperture Sensorcraft", *49th AIAA Structures, Structural Dynamics, and Materials Conference,* Schaumburg, IL.

[7] Fang, J., and Lyons, G. J., 1996, "Structural Damping of tensioned Pipes with Reference to Cables", *Journal of Sound and Vibration*, **194**(3), pp.891-907.

[8] Winslow, C., 1993 "Space Station Freedom Solar Array Design Development", *IEEE Aerospace and Electronic Systems Magazine*, **8**(1), pp. 3-8.

[9] Kemerley, R. T., and Kiss, S., 2000 "Advanced Technology for Future Space-Based Antennas", *IEEE MTT-S International Microwave Symposium Digest*, Boston, MA, pp.717-720.

[10] Onoda, J., Endo, T., Tamaoki, H., and Watanabe, N., 1991, "Vibration Suppression by Variable-Stiffness Members", *AIAA Journal*, **29**(6), pp.977-983.

[11] Onoda, J., Sano, T., and Kamiyama, K., 1992, "Active, Passive, and Semiactive Vibration Suppression by Stiffness Variation", *AIAA Journal*, **30**(12), pp.2922-2929.

[12] Clark, W. W., 2000, "Vibration Control with State-Switching Piezoelectric Materials", *Journal of Intelligent Material Systems and Structures*, **11**(4), pp.263-271.

[13] Corr, L. R., and Clark, W. W., 2001, "Energy Dissipation Analysis of Piezoceramic Semiactive Vibration Control", *Journal of Intelligent Material Systems and Structures*, **12**(11), pp.729-736.

[14] Ramaratnam, A. and Jalili, N., 2006, "A Switched Stiffness Approach for Structural Vibration Control: Theory and Real-Time Implementation", *Journal of Sound and Vibration*, **291**(1-2), pp.258-274.

[15] Diaz, A. R., and Mukherjee, R., 2006, "Topology Optimization Problem in Control of Structures using Modal Disparity", *ASME Journal of Mechanical Design*, **128**(3), pp.536-541.

[16] Diaz, A. R., and Mukherjee, R., 2008, "Optimal Joint Placement and Modal Disparity in Control of Flexible Structures", *Computers and Structures*, **86**(13-14), pp. 1456-1462.

[17] Issa. J., Mukherjee, R., and Diaz, A. R., 2009, "Energy Dissipation in Dynamical Systems Through Sequential Application and Removal of Constraints", *ASME Journal of Dynamic Systems, Measurement and Control*, **131**(2).

[18] Perkins. N. C., 1990, "Planar Vibration of an Elastica Arch - Theory and Experiment", *ASME Journal of Vibration and Acoustics* **112**(3), pp.374-379.

[19] Perkins. N. C., and Mote, C. D., Jr., 1987, "Three Dimensional Vibration of a Translating Elastic Cable", *Journal of Sound and Vibration*, **114**(2), pp. 325-340.

[20] Diaz, A. R., and Mukherjee, R., 2006, "Modal Disparity Enhancement through Optimal insertion of Nonstructural Masses", *Structural and Multidiscilinary Optimization*, **31**(1), pp.1-7.

[21] Issa. J., Mukherjee, R., Diaz, A. R., and Shaw, S. W., 2008, "Modal Disparity and its Experimental Verification", *Journal of Sound and Vibration*, **311**(3-5), pp.1465-1475.